

UCSF

UC San Francisco Previously Published Works

Title

A repository of grade 1 and 2 meningioma MRIs in a public dataset for radiomics reproducibility tests.

Permalink

<https://escholarship.org/uc/item/04c9h8s6>

Journal

Medical Physics, 51(3)

Authors

Vasantachart, April

Cao, Yufeng

Shen, Zhilei

et al.

Publication Date

2024-03-01

DOI

10.1002/mp.16763

Peer reviewed



Published in final edited form as:

Med Phys. 2024 March ; 51(3): 2334–2344. doi:10.1002/mp.16763.

A repository of grade 1 and 2 meningioma MRIs in a public dataset for radiomics reproducibility tests

April Vasantachart^{1,2}, Yufeng Cao², Zhilei Shen², Karen Cheng^{1,2}, Michael Gribble³, Jason C. Ye², Gabriel Zada⁴, Kyle Hurth⁵, Anna Mathew⁵, Samuel Guzman⁵, Wensha Yang²

¹Department of Radiation Oncology, LAC+USC Medical Center, Los Angeles, California, USA

²Department of Radiation Oncology, Keck School of Medicine, University of Southern California, Los Angeles, California, USA

³Keck School of Medicine, University of Southern California, Los Angeles, California, USA

⁴Department of Neurological Surgery, Keck School of Medicine, University of Southern California, Los Angeles, California, USA

⁵Department of Pathology, Keck School of Medicine, University of Southern California, Los Angeles, California, USA

Abstract

Purpose: Meningiomas are the most common primary brain tumors in adults with management varying widely based on World Health Organization (WHO) grade. However, there are limited datasets available for researchers to develop and validate radiomic models. The purpose of our manuscript is to report on the first dataset of meningiomas in The Cancer Imaging Archive (TCIA).

Acquisition and validation methods: The dataset consists of pre-operative MRIs from 96 patients with meningiomas who underwent resection from 2010–2019 and include axial T1post and T2-FLAIR sequences—55 grade 1 and 41 grade 2. Meningioma grade was confirmed based on the 2016 WHO Bluebook classification guideline by two neuropathologists and one neuropathology fellow. The hyperintense T1post tumor and hyperintense T2-FLAIR regions were manually contoured on both sequences and resampled to an isotropic resolution of $1 \times 1 \times 1 \text{ mm}^3$. The entire dataset was reviewed by a certified medical physicist.

Data format and usage notes: The data was imported into TCIA for storage and can be accessed at <https://doi.org/10.7937/OTKV-1A36>. The total size of the dataset is 8.8GB, with 47 519 individual Digital Imaging and Communications in Medicine (DICOM) files consisting of 384 image series, and 192 structures.

Potential applications: Grade 1 and 2 meningiomas have different treatment paradigms and are often treated based on radiologic diagnosis alone. Therefore, predicting grade prior to treatment

Correspondence: April Vasantachart, City of Hope Sherman Oaks, 5522 Sepulveda Boulevard, Sherman Oaks, CA 91411, USA., aprilkeiko@gmail.com.

CONFLICT OF INTEREST STATEMENT

The authors declare no conflicts of interest.

is essential in clinical decision-making. This dataset will allow researchers to create models to auto-differentiate grade 1 and 2 meningiomas as well as evaluate for other pathologic features including mitotic index, brain invasion, and atypical features. Limitations of this study are the small sample size and inclusion of only two MRI sequences. However, there are no meningioma datasets on TCIA and limited datasets elsewhere although meningiomas are the most common intracranial tumor in adults.

Keywords

atypical; dataset; meningioma; radiomics; TCIA

1 | INTRODUCTION

Meningiomas are the most common primary brain tumors in adults, representing 40% of all primary brain tumors, with approximately 41 000 new cases per year in the United States.¹ Meningiomas are further classified into World Health Organization (WHO) grade 1, 2, and 3 according to the 2021 WHO classification system.² The majority of meningiomas are diagnosed radiologically with no pathologic confirmation or knowledge of the pathologic grade.³ However, the recommended course of treatment for meningiomas can range from observation to surgical resection with adjuvant radiation based on grade.^{4,5} Therefore, accurate grading of meningiomas is critical for predicting disease courses and facilitating clinical decision-making.

Radiomics is a quantitative approach to medical imaging in which large amounts of image features are extracted from regions of interest in medical images. Recent studies in oncological imaging have highlighted the potential of radiomics to predict tumor grading in multiple cancers, including central nervous system tumors such as gliomas.⁶ Likewise, radiomic features have the potential to predict meningioma grade. Magnetic Resonance Imaging (MRI) is the modality of choice in assessing meningiomas, and deep learning models have been developed for auto-differentiation of grade.⁷⁻¹⁰ However, there are limited datasets available for researchers to develop and validate radiomic models. Furthermore, in the limited and small datasets available, thorough pathologic evaluation is unclear and there is a low representation of grade 2 meningiomas. Our group has previously published on auto-differentiation of grade 1 and 2 meningiomas utilizing an asymmetric 3D convolutional neural network (CNN) architecture using two encoding paths based on the T1post and T2-FLAIR MRIs. The model was trained and tested on 96 patients (random rotation was used for data augmentation and assessed by tenfold cross-validation, with each fold consisting of randomly selected 10 testing, 76 training, and 10 validation subjects) and showed improved grading accuracy using both T1post and T2-FLAIR MRIs with accuracy rates of 90%.¹⁰ Previous studies using a single sequence MRI showed reduced accuracy,⁷⁻⁹ highlighting the importance of sharing datasets with the community to allow researchers to train models with new datasets and multiple MRI sequences.

The purpose of this publication is to report on the first dataset of meningiomas in The Cancer Imaging Archive (TCIA). The importance of reproducibility and validation studies utilizing radiomic models continues to grow and the addition of our public dataset will

allow for training new models, validating prior models, and collaborative efforts among institutions.

2 | ACQUISITION AND VALIDATION METHODS

2.1 | Overview of the dataset

The dataset consists of pre-operative MRIs for 96 patients with meningiomas who underwent resection (subtotal or gross total) from 2010 to 2019. The MRIs include axial T1post and T2-FLAIR sequences of 55 grade 1 and 41 grade 2 meningiomas. Pathology was confirmed based on the 2016 WHO Bluebook classification guidelines¹¹ by a neuropathology team that included two subspecialty trained neuropathologists and one neuropathology fellow. The images were collected for a previously published study on auto-differentiation of grade 1 and 2 meningiomas using an asymmetric CNN¹⁰ and the study was approved by the institutional review board (IRB) to review human subjects research (protocol ID HS-18-00261) at the University of Southern California. The auto-differentiation code can be reviewed and accessed on <https://github.com/usc2021/YCWWYAV>. TABLE 1 includes the age, sex, type of resection, and pathologic characteristics of the 96 included patients.

2.2 | Acquisition

MRI scanners from different vendors were used and included 1.5 or 3T GE (OptimaTM, DiscoveryTM, SignaTM), Philips (AchievaTM, InteraTM), Siemens (SymphonyTM, SkyraTM), Toshiba (TitanTM, MRT 200TM, GalanTM), and Hitachi (OasisTM, EchelonTM). The scanning parameters for the T1post sequence included a TR of 7–8 ms, a TE of 2–3 ms, an isotropic in-plane spatial resolution of 1.016 mm, an in-plane volumetric dimension of 256×256 , a slice thickness of 1–2 mm, a FOV of 100 mm^2 , and a flip angle of 15° . The scanning parameters for the T2-FLAIR include a TR of 8000–11000 ms, a TE of 120–159 ms, an isotropic in-plane resolution of 0.4–0.9 mm, an in-plane volumetric dimension of $256\text{--}512 \times 256\text{--}512$, a slice thickness of 2–7 mm, a FOV of $80\text{--}100 \text{ mm}^2$, and a flip angle of $90\text{--}180^\circ$.

The T1post and T2-FLAIR MRIs for each patient were acquired in the same study. The DICOM files containing the T1post and T2-FLAIR MRIs were exported to VelocityAITM (Varian, Palo Alto, CA). The original DICOM registration was reviewed by overlaying the two images and inspecting the alignment of the skull and ventricles. If the alignment was off, we performed an automatic rigid registration using the mutual information algorithm installed on VelocityAITM.

2.3 | Segmentation

The hyperintense T1post tumor and hyperintense T2-FLAIR region were manually contoured on each image by a medical student and radiation oncology resident, and reviewed by a radiation oncologist with over 5 years of experience as shown in Figure 1. The organized dataset, including original MRIs, was resampled to an isotropic resolution of $1 \times 1 \times 1 \text{ mm}^3$.

2.4 | Data format and usage notes

The MRIs were exported from Synapse and the contours were exported from VelocityAI™. The data was then imported into TCIA at the National Institutes of Health¹² for storage where post-processing was completed to ensure all potentially confidential data was removed. The images, registration, and contours were stored under an anonymized patient identifier with clinical data as seen in TABLE 1. The dataset can be found on <http://www.cancerimagingarchive.net/> under the title “Segmentation and Classification of Grade I and II Meningiomas from MRI: an Open Annotated Dataset (Meningioma-SEG-CLASS)”.¹³ Alternatively, the dataset can also be accessed by digital object identifier (DOI) <https://doi.org/10.7937/0TKV-1A36>. The total size of the dataset is 8.8GB, with 47 519 individual DICOM files consisting of 384 image series, and 192 structures. DICOM compatibility has been tested with Eclipse and Machine Identity Management (MIM) (MIM Software, Cleveland, OH, USA).

2.5 | Data validation

The entire dataset (96 patients) including the MRIs, registrations, and contours, has been reviewed by a certified medical physicist. The compatibility of the dataset has been tested with Eclipse and MIM (MIM Software, Cleveland, OH, USA).

3 | DISCUSSION

This dataset includes a repository of grade 1 and 2 meningioma with contours on both T1post and T2-FLAIR MRIs. There are no meningioma datasets within TCIA and limited public datasets available, particularly for grade 2 meningiomas that have been pathologically graded based on the WHO 2016 criteria. This dataset will allow researchers to create models to auto-differentiate grade 1 and 2 meningiomas as well as evaluate for other pathologic features including mitotic index, brain invasion, and atypical features. Additionally, this dataset could be used to validate other models published previously on auto-differentiation of grade 1 and 2 meningiomas and potentiate multi-institutional validation studies for the use of radiomics to pre-operatively determine pathologic features of meningiomas.

As grade 1 and 2 meningiomas have different treatment paradigms and are often treated based on radiologic diagnosis alone, predicting grade prior to treatment is essential in clinical decision-making. Earlier stratification of meningioma grade has the potential to effect surveillance patterns for patients on observation with low grade disease and instigate trials assessing for escalation of treatment for those predicted to have high grade disease. Limitations of this study are the small sample size and inclusion of only two MRI sequences. However, there are no meningioma datasets on TCIA and limited datasets elsewhere although meningiomas are the most common intracranial tumor in adults. Our pathologic evaluation did not include molecular analyses and although grade 3 meningiomas are rare, TERT promoter and CDKN2A/B would upgrade meningiomas to grade 3 based on the 2021 WHO classification system.²

Prediction of meningioma grade is important in the management of meningiomas and has the potential to affect a wide population due to the high incidence of meningiomas. Giving

researchers access to datasets will allow for improved radiomic studies of this common but understudied tumor.

4 | CONCLUSION

This manuscript describes a repository of grade 1 and 2 meningiomas with pre-operative T1post and T2-FLAIR MRIs and is the first cohort of meningioma patients in the TCIA.

ACKNOWLEDGMENTS

The authors have nothing to report.

REFERENCES

- Ostrom QT, Price M, Neff C, et al. CBTRUS statistical report: primary brain and other central nervous system tumors diagnosed in the United States in 2015–2019. *Neuro Oncol.* 2022;24(5):v1–v95. doi:10.1093/neuonc/noac202 [PubMed: 36196752]
- Louis DN, Perry A, Wesseling P, et al. The 2021 WHO classification of tumors of the central nervous system: a summary. *Neuro Oncol.* 2021;23(8):1231–1251. doi:10.1093/neuonc/noab106 [PubMed: 34185076]
- Buerki RA, Horbinski CM, Kruser T, Horowitz PM, James CD, Lukas RV. An overview of meningiomas. *Futur Oncol.* 2018;14(21):2161–2177. doi:10.2217/fon-2018-0006
- Rogers L, Zhang P, Vogelbaum MA, et al. Intermediate-risk meningioma: initial outcomes from NRG oncology RTOG 0539. *J Neurosurg.* 2018;129(1):35–47. doi:10.3171/2016.11.JNS161170 [PubMed: 28984517]
- Rogers L, Zhang P, Vogelbaum MA, et al. Intermediate-risk meningioma: initial outcomes from NRG oncology RTOG 0539. *J Neurosurg.* 2018;129(1):35–47. doi:10.3171/2016.11.JNS16117 [PubMed: 28984517]
- Pyka T, Gempt J, Hiob D, et al. Textural analysis of pre-therapeutic [18F]-FET-PET and its correlation with tumor grade and patient survival in high-grade gliomas. *Eur J Nucl Med Mol Imaging.* 2016;43(1):133–141. doi:10.1007/s00259-015-3140-4 [PubMed: 26219871]
- Banzato T, Causin F, Della Puppa A, Cester G, Mazzai L, Zotti A. Accuracy of deep learning to differentiate the histopathological grading of meningiomas on MR images: a preliminary study. *J Magn Reson Imaging.* 2019;50(4):1152–1159. doi:10.1002/jmri.26723 [PubMed: 30896065]
- Zhu Y, Man C, Gong L, et al. A deep learning radiomics model for preoperative grading in meningioma. *Eur J Radiol.* 2019;116:128–134. doi:10.1016/j.ejrad.2019.04.02 [PubMed: 31153553]
- Zhang H, Mo J, Jiang H, et al. Deep learning model for the automated detection and histopathological prediction of meningioma. *Neuroinformatics.* 2021;19(3):393–402. doi:10.1007/s12021-020-09492-6 [PubMed: 32974873]
- Vasantachart A, Cao Y, Gribble M, et al. Automatic differentiation of grade I and II meningiomas on magnetic resonance image using an asymmetric convolutional neural network. *Sci Rep.* 2022;12(1):3806. doi:10.1038/s41598-022-07859-0 [PubMed: 35264655]
- Louis DN, Perry A, Reifenberger G, et al. The 2016 world health organization classification of tumors of the central nervous system: a summary. *Acta Neuropathol.* 2016;131(6):803–820. doi:10.1007/s00401-016-1545-1 [PubMed: 27157931]
- Clark K, Vendt B, Smith K, et al. The Cancer Imaging Archive (TCIA): maintaining and operating a public information repository. *J Digit Imaging.* 2013;26(6):1045–1057. doi:10.1007/s10278-013-9622-7 [PubMed: 23884657]
- Vasantachart A, Cao Y, Shen Z, et al. Segmentation and classification of grade I and II meningiomas from magnetic resonance imaging: an open annotated dataset (Meningioma-SEG-CLASS). *Cancer Imaging Arch.* 2023. doi:10.7937/OTKV-1A36

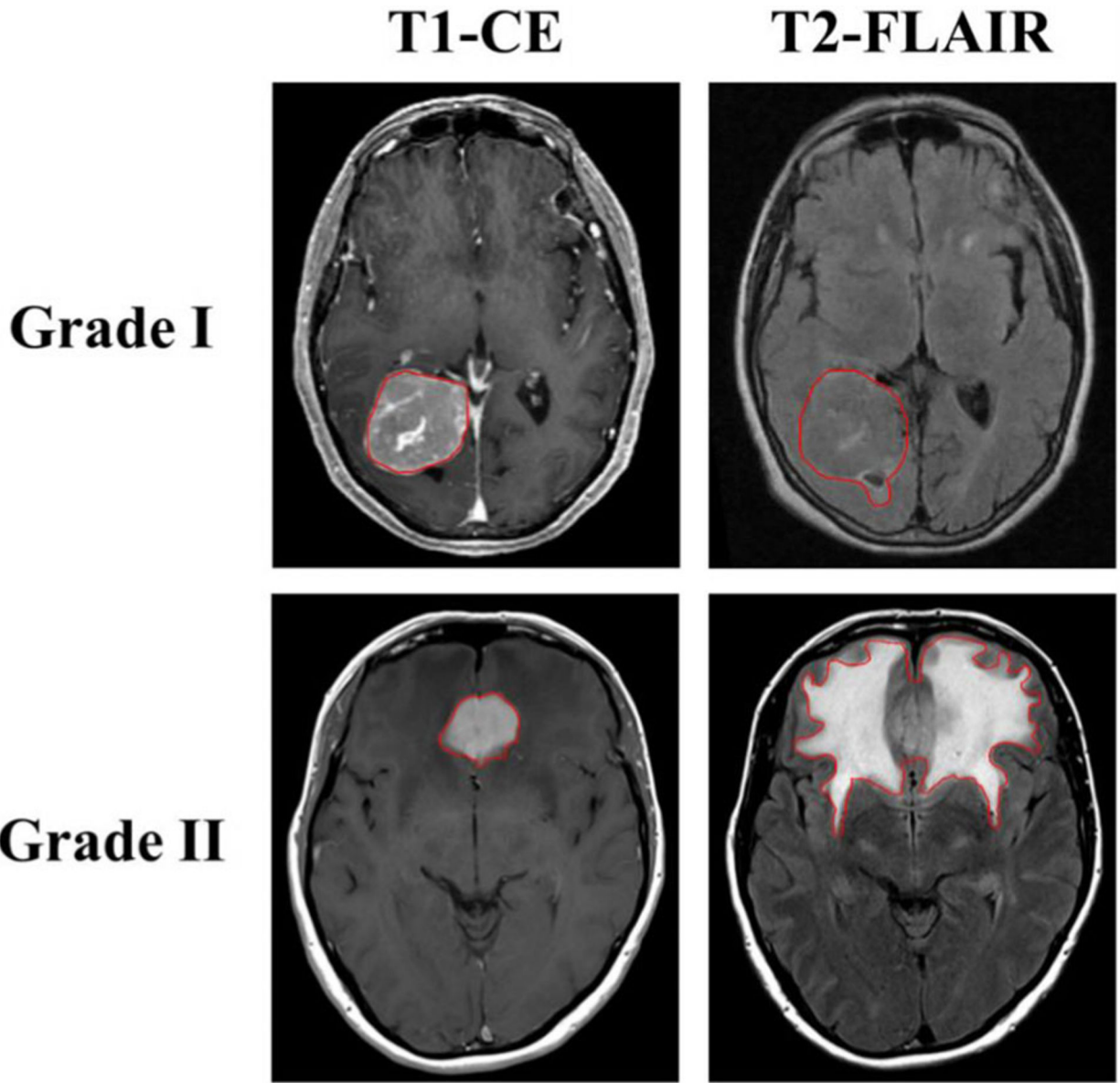


FIGURE 1.
Examples of grade 1 and 2 meningioma contours on T1-CE and T2-FLAIR.

TABLE 1

Patient age, sex, type of resection, and pathologic grade.

Patient	Age	Sex	Resection type	Pathologic grade	Subtype	Atypical features	Brain invasion	Mitotic count	Grouped location
Meningioma-SEG-CLASS-001	67	F	GTR	II	Atypical	Sheeting	N	4 per 10 hpf	Convexity
Meningioma-SEG-CLASS-002	82	F	STR	II	Atypical	Hypercellular Macronucleoli Small cells	N	5 per 10 hpf	Falx & Parasagittal
Meningioma-SEG-CLASS-003	83	F	GTR	I	Meningothelial	N	N	Rare	Middle Cranial Fossa
Meningioma-SEG-CLASS-004	57	F	GTR	I	Meningothelial	N	N	Rare	Convexity
Meningioma-SEG-CLASS-005	42	F	GTR	I	Secretory	N	N	None	Middle Cranial Fossa
Meningioma-SEG-CLASS-006	57	M	GTR	I	Meningothelial	N	N	Rare	Middle Cranial Fossa
Meningioma-SEG-CLASS-007	74	F	GTR	II	Atypical	Hypercellular Macronucleoli Small cells with high Nuclear:Cytoplasm ratio	N	None	Falx & Parasagittal
Meningioma-SEG-CLASS-008	33	F	GTR	II	Atypical	Hypercellular	N	4 per 10 hpf	Convexity
Meningioma-SEG-CLASS-009	61	M	STR	II	Atypical	N	N	6 per 10 hpf	Middle Cranial Fossa
Meningioma-SEG-CLASS-010	56	F	STR	I	Meningothelial	N	N	Rare	Middle Cranial Fossa
Meningioma-SEG-CLASS-011	54	F	STR	I	Meningothelial	N	N	Rare	Middle Cranial Fossa
Meningioma-SEG-CLASS-012	81	F	GTR	I	Meningothelial	N	N	Rare	Falx & Parasagittal
Meningioma-SEG-CLASS-013	88	F	GTR	II	Atypical	Hypercellular Macronucleoli Small cells with high Nuclear:Cytoplasm ratio	N	4 per 10 hpf	Convexity
Meningioma-SEG-CLASS-014	55	M	GTR	II	Atypical	N	N	6 per 10 hpf	Convexity
Meningioma-SEG-CLASS-015	77	M	GTR	II	Mixed (Atypical, Chordoid, Clear cell)	Sheeting Hypercellularity	N	Rare	Falx & Parasagittal
Meningioma-SEG-CLASS-016	71	F	GTR	I	Meningothelial	N	N	None	Middle Cranial Fossa
Meningioma-SEG-CLASS-017	64	M	STR	I	Meningothelial	N	N	Rare	Middle Cranial Fossa

Patient	Age	Sex	Resection type	Pathologic grade		Subtype	Atypical features	Brain invasion	Mitotic count	Grouped location
				type	grade					
Meningioma-SEG-CLASS-018	60	F	GTR	I		Meningothelial	N	N	None	Middle Cranial Fossa
Meningioma-SEG-CLASS-019	38	F	STR	I		Meningothelial	N	N	None	Posterior Cranial Fossa
Meningioma-SEG-CLASS-020	55	F	GTR	I		Meningothelial	N	N	None	Middle Cranial Fossa
Meningioma-SEG-CLASS-021	61	M	GTR	II		Atypical	Sheeting Hypercellularity Small Cells with high Nuclear: Cytoplasm ratio	N	5 per 10 hpf	Falx & Parasagittal
Meningioma-SEG-CLASS-022	37	F	GTR	I		Meningothelial	N	N	Rare	Lateral Ventricle
Meningioma-SEG-CLASS-023	39	F	STR	I		Meningothelial	N	N	1 per 10 hpf	Posterior Cranial Fossa
Meningioma-SEG-CLASS-024	56	M	GTR	I		Meningothelial	N	N	None	Middle Cranial Fossa
Meningioma-SEG-CLASS-025	74	M	STR	I		Secretory	N	N	2 per 10 hpf	Middle Cranial Fossa
Meningioma-SEG-CLASS-026	85	M	STR	II		Chordoid	N	N	Rare	Middle Cranial Fossa
Meningioma-SEG-CLASS-027	51	F	STR	I		Meningothelial	N	N	Rare	Middle Cranial Fossa
Meningioma-SEG-CLASS-028	47	F	GTR	I		Meningothelial	N	N	Rare	Anterior Cranial Fossa
Meningioma-SEG-CLASS-029	66	M	STR	II		Atypical	Hypercellularity Necrosis	Y	4 per 10 hpf	Falx & Parasagittal
Meningioma-SEG-CLASS-030	59	F	STR	I		Meningothelial	N	N	Rare	Falx & Parasagittal
Meningioma-SEG-CLASS-031	55	F	GTR	II		Chordoid	N	Y	Rare	Anterior Cranial Fossa
Meningioma-SEG-CLASS-032	64	F	GTR	II		Atypical	Necrosis Hypercellularity Sheetting Small cells	Y	Rare	Falx & Parasagittal
Meningioma-SEG-CLASS-033	46	M	GTR	I		Meningothelial	N	N	1 per 10 hpf	Middle Cranial Fossa
Meningioma-SEG-CLASS-034	74	F	STR	II		Atypical	Necrosis Hypercellularity Sheetting Small cells	N	5 per 10 hpf	Middle Cranial Fossa
Meningioma-SEG-CLASS-035	47	F	GTR	I		Meningothelial	N	N	None	Posterior Cranial Fossa
Meningioma-SEG-CLASS-036	42	F	GTR	I		Psammomatous	N	N	None	Falx & Parasagittal

Patient	Age	Sex	Resection type	Pathologic grade		Subtype	Atypical features	Brain invasion	Mitotic count	Grouped location
				type	grade					
Meningioma-SEG-CLASS-037	72	F	GTR	I		Meningothelial	N	N	None	Middle Cranial Fossa
Meningioma-SEG-CLASS-038	56	F	GTR	I		Meningothelial	N	N	None	Middle Cranial Fossa
Meningioma-SEG-CLASS-039	44	F	GTR	I		Meningothelial	N	N	Rare	Posterior Cranial Fossa
Meningioma-SEG-CLASS-040	56	F	GTR	I		Meningothelial	N	N	Rare	Middle Cranial Fossa
Meningioma-SEG-CLASS-041	61	M	STR	II		Atypical	N	N	4 per 10 hpf	Convexity
Meningioma-SEG-CLASS-042	60	F	GTR	I		Meningothelial	N	N	Rare	Falx & Parasagittal
Meningioma-SEG-CLASS-043	50	F	GTR	I		Fibrous	N	N	Rare	Posterior Cranial Fossa
Meningioma-SEG-CLASS-044	61	F	STR	I		Meningothelial	N	N	None	Middle Cranial Fossa
Meningioma-SEG-CLASS-045	65	F	GTR	II		Atypical	Small cells Macronucleoli	N	4 per 10 hpf	Anterior Cranial Fossa
Meningioma-SEG-CLASS-046	32	F	STR	I		Meningothelial	N	N	None	Middle Cranial Fossa
Meningioma-SEG-CLASS-047	64	F	GTR	I		Meningothelial	N	N	Rare	Falx & Parasagittal
Meningioma-SEG-CLASS-048	66	M	STR	II		Atypical	Hypercellular Small cells Necrosis	Y	6 per 10 hpf	Middle Cranial Fossa
Meningioma-SEG-CLASS-049	31	F	GTR	I		Meningothelial	N	N	Rare	Middle Cranial Fossa
Meningioma-SEG-CLASS-050	56	F	GTR	II		Atypical	N	Y	None	Convexity
Meningioma-SEG-CLASS-051	52	M	GTR	II		Atypical	Necrosis Small cells Hypercellular	N	5 per 10 hpf	Middle Cranial Fossa
Meningioma-SEG-CLASS-052	75	F	GTR	I		Meningothelial	Necrosis (rare)	N	None	Posterior Cranial Fossa
Meningioma-SEG-CLASS-053	50	F	STR	I		Meningothelial	Small cells Macronucleoli	N	Rare	Middle Cranial Fossa
Meningioma-SEG-CLASS-054	49	M	GTR	I		Meningothelial	N	N	Rare	Anterior Cranial Fossa
Meningioma-SEG-CLASS-055	39	F	STR	I		Meningothelial	N	N	Rare	Posterior Cranial Fossa

Patient	Age	Sex	Resection type	Pathologic grade		Subtype	Atypical features	Brain invasion	Mitotic count	Grouped location
				type	grade					
Meningioma-SEG-CLASS-056	48	F	STR	I	I	Meningothelial	N	N	None	Middle Cranial Fossa
Meningioma-SEG-CLASS-057	57	F	STR	II	II	Atypical	N	N	4 per 10 hpf	Middle Cranial Fossa
Meningioma-SEG-CLASS-058	46	F	GTR	I	I	Meningothelial	Hypercellular Small cells	N	Rare	Middle Cranial Fossa
Meningioma-SEG-CLASS-059	54	F	GTR	I	I	Meningothelial	N	N	Rare	Lateral Ventricle
Meningioma-SEG-CLASS-060	69	M	GTR	II	II	Atypical	Sheeting Hypercellular Necrosis Macronucleoli	Y	6 per 10 hpf	Falx & Parasagittal
Meningioma-SEG-CLASS-061	58	F	GTR	I	I	Meningothelial	N	N	2 per 10 hpf	Convexity
Meningioma-SEG-CLASS-062	59	M	STR	II	II	Atypical	Small cells with high Nuclear:Cytoplasm ratio Macronucleoli	Y	Rare	Posterior Cranial Fossa
Meningioma-SEG-CLASS-063	35	F	GTR	II	II	Atypical	N	N	4 per 10 hpf	Middle Cranial Fossa
Meningioma-SEG-CLASS-064	46	M	GTR	II	II	Atypical	Small cells Hypercellular Macronucleoli	N	5 per 10 hpf	Convexity
Meningioma-SEG-CLASS-065	64	F	GTR	I	I	Meningothelial	N	N	None	Middle Cranial Fossa
Meningioma-SEG-CLASS-066	50	F	STR	I	I	Meningothelial	N	N	2 per 10 hpf	Anterior Cranial Fossa
Meningioma-SEG-CLASS-067	55	F	STR	I	I	Meningothelial	N	N	Rare	Middle Cranial Fossa
Meningioma-SEG-CLASS-068	50	F	STR	I	I	Meningothelial	N	N	Rare	Falx & Parasagittal
Meningioma-SEG-CLASS-069	72	M	GTR	II	II	Chordoid	N	N	Rare	Convexity
Meningioma-SEG-CLASS-070	72	M	STR	II	II	Atypical	Hypercellular Sheetting Necrosis Macronucleoli	N	7 per 10 hpf	Convexity
Meningioma-SEG-CLASS-071	66	F	GTR	II	II	Atypical	Hypercellular Macronucleoli Small cells	N	Rare	Convexity
Meningioma-SEG-CLASS-072	55	F	STR	I	I	Secretory	N	N	None	Posterior Cranial Fossa
Meningioma-SEG-CLASS-073	50	F	GTR	II	II	Atypical	Hypercellular Small cells	N	4 per 10 hpf	Middle Cranial Fossa
Meningioma-SEG-CLASS-074	37	F	STR	I	I	Meningothelial	N	N	Rare	Middle Cranial Fossa

Patient	Age	Sex	Resection type	Pathologic grade		Subtype	Atypical features	Brain invasion	Mitotic count	Grouped location
				type	grade					
Meningioma-SEG-CLASS-075	29	M	STR	II	II	Atypical	Hypercellular Small cells Necrosis	N	2 per 10 hpf	Falx & Parasagittal
Meningioma-SEG-CLASS-076	37	M	GTR	II	II	Atypical	Hypercellular	N	4 per 10 hpf	Convexity
Meningioma-SEG-CLASS-077	36	F	GTR	I	I	Meningothelial	N	N	2 per 10 hpf	Falx & Parasagittal
Meningioma-SEG-CLASS-078	64	M	GTR	II	II	Atypical	N	N	2 per 10 hpf	Convexity
Meningioma-SEG-CLASS-079	37	M	STR	I	I	Meningothelial	N	N	None	Anterior Cranial Fossa
Meningioma-SEG-CLASS-080	53	F	GTR	II	II	Atypical	Clear cell	Y	6-8 per 10 hpf	Convexity
Meningioma-SEG-CLASS-081	53	F	GTR	II	II	Atypical	Hypercellular Small cells	N	4 per 10 hpf	Convexity
Meningioma-SEG-CLASS-082	25	F	STR	I	I	Meningothelial	N	N	Rare	Falx & Parasagittal
Meningioma-SEG-CLASS-083	64	F	GTR	I	I	Meningothelial	N	N	None	Middle Cranial Fossa
Meningioma-SEG-CLASS-084	61	M	GTR	II	II	Atypical	Hypercellular Small cells Necrosis	Y	7 per 10 hpf	Convexity
Meningioma-SEG-CLASS-085	38	F	STR	II	II	Atypical	N	N	4 per 10 hpf	Middle Cranial Fossa
Meningioma-SEG-CLASS-086	67	F	STR	II	II	Atypical	Small cells Macronucleoli Necrosis	Y	6 per 10 hpf	Falx & Parasagittal
Meningioma-SEG-CLASS-087	47	M	GTR	II	II	Atypical	N	Y	4 per 10 hpf	Convexity
Meningioma-SEG-CLASS-088	67	F	STR	II	II	Atypical	N	N	5 per 10 hpf	Middle Cranial Fossa
Meningioma-SEG-CLASS-089	43	F	GTR	I	I	Secretory	N	N	Rare	Posterior Cranial Fossa
Meningioma-SEG-CLASS-090	44	F	GTR	II	II	Atypical	Hypercellular Small cells with high Nuclear:Cytoplasm ratio	N	Rare	Middle Cranial Fossa
Meningioma-SEG-CLASS-091	41	F	GTR	I	I	Meningothelial	Hypercellular Small cells	N	2 per 10 hpf	Posterior Cranial Fossa
Meningioma-SEG-CLASS-092	77	M	GTR	II	II	Atypical	Small cells Macronucleoli Necrosis	N	9 per 10 hpf	Convexity
Meningioma-SEG-CLASS-093	59	F	STR	I	I	Meningothelial	N	N	Rare	Posterior Cranial Fossa

Patient	Age	Sex	Resection type	Pathologic grade	Subtype	Atypical features	Brain invasion	Mitotic count	Grouped location
Meningioma-SEG-CLASS-094	72	M	GTR	I	Secretory	N	N	Rate	Convexity
Meningioma-SEG-CLASS-094	72	M	GTR	II	Atypical	N	N	4 per 10 hpf	Convexity
Meningioma-SEG-CLASS-095	72	F	STR	II	Atypical	N	Y	2 per 10 hpf	Middle Cranial Fossa
Meningioma-SEG-CLASS-096	30	M	GTR	II	Atypical	Hypercellular Small cells with high Nuclear:Cytoplasm ratio	N	2 per 10 hpf	Middle Cranial Fossa